Effects of crop residue incorporation and properties on combined soil gaseous N_2O, NO, and NH_3 emissions—A laboratory-based measurement approach

Baldur Janz [a,*,1], Felix Havermann [a,1,2,3], Gwenaëlle Lashermes [b], Pablo Zuazo [a,2], Florian Engelsberger [a], Seyedeh Mahsa Torabi [a], Klaus Butterbach-Bahl [a]

[a] Karlsruhe Institute of Technology, Institute of Meteorology and Climate Research–Atmospheric Environmental Research, Garmisch-Partenkirchen, Germany
[b] Université de Reims Champagne Ardenne, INRAE, FARE, UMR A 614, 51097 Reims, France

HIGHLIGHTS

- Simultaneous quantification of N losses (N_2O, NO, NH_3) during residue decomposition.
- Range of residue N emission factor for N_2O (EF_{N2O}) exceeds IPCC value.
- Total residue N or residue C/N ratio does not explain EF_{N2O} variability.
- Residue properties (e.g., soluble, lignin) control potential N trace gas emissions.
- N trace gas emissions decreased as physiological stage of residues increased.

GRAPHICAL ABSTRACT
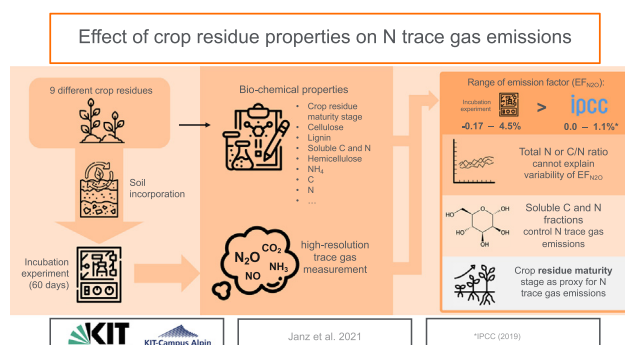
ARTICLE INFO

ABSTRACT

Crop residues may serve as a significant source of soil emissions of N_2O and other trace gases. According to the emission factors (EFs) set by the Intergovernmental Panel on Climate Change (IPCC), N_2O emission is proportional to the amount of N added by residues to the soil. However, the effects of crop residues on the source and sink strength of agroecosystems for trace gases are regulated by their properties, such as the C and N content; C/N ratio; lignin, cellulose, and soluble fractions; and residue humidity. In the present study, an automated dynamic chamber method was used in combination with soil mesocosms to simultaneously measure the effects of nine different crop residues (oilseed rape, winter wheat, field pea, maize, potato, mustard, red clover, sugar beet, and ryegrass) on soil respiration (CO_2) and reactive N fluxes (N_2O, NO, and NH_3) at a high temporal resolution. Specifically, crop residues were incorporated in the 0–4 cm topsoil layer and incubated for 60 days at a constant temperature (15 °C) and water-filled pore space (60% WFPS). Residue incorporation immediately and sharply increased soil N_2O and CO_2 emissions, but these were short-lived and returned to background levels within respectively 10 and 30 days. The magnitude of increase in soil NO flux following residue incorporation was lower than that in CO_2 and N_2O fluxes, with peak emissions observed around day 20. Overall, the N content or C/N ratio of the applied residue could not sufficiently explain the variation in soil N_2O and NO emissions. The range of

* Corresponding author.
  E-mail address: baldur.janz@kit.edu (B. Janz).
[1] Baldur Janz and Felix Havermann contributed equally to the manuscript and should be considered as joint first authors.
[2] Formerly at: Karlsruhe Institute of Technology, Institute of Meteorology and Climate Research–Atmospheric Environmental Research, Garmisch-Partenkirchen, Germany.
[3] Now at: Ludwig-Maximilians-Universität München, Department of Geography, Munich, Germany.

the calculated N_2O EFs over a 60-day period was -0.17 to $+4.5$, being wider than that proposed by the IPCC ($+0.01$ to $+1.1$). Therefore, the residue maturity stage may be used as a simple proxy to estimate the $N_2O + NO$ emissions from incorporated residue.

© 2021 Published by Elsevier B.V.

1. Introduction

Crop residue incorporation in soils is a key practice in agricultural management. Residues provide organic C and N inputs to soils for maintaining or improving the soil stocks of these elements and, ultimately, soil health and crop productivity (Lehtinen et al., 2014; Liu et al., 2014; Lugato et al., 2014). However, residue decomposition may result in the formation of the hotspots of microbial N turnover processes (Kuzyakov and Blagodatskaya, 2015) and significant losses of reactive N compounds from soils (Baggs et al., 2000). In particular, the environmentally relevant reactive gaseous N forms emitted from the incorporated residue include the potent greenhouse gas (GHG) nitrous oxide (N_2O), the tropospheric ozone-depleting gas nitric oxide (NO) (Pilegaard, 2013), and the aerosol-forming and eutrophicating gases ammonia (NH_3) (Nemitz et al., 2009) and nitrate (NO_3^-), which may be leached from soils to water resources.

Agriculture accounts for 59%–66% of global anthropogenic N_2O emissions and 10% of anthropogenic NO emissions (Butterbach-Bahl et al., 2009; Ciais et al., 2013; IPCC, 2019a). National GHG inventories typically estimate N_2O emissions from croplands based on emission factors (EFs), as outlined by the Intergovernmental Panel on Climate Change (IPCC, 2006, 2019b). Briefly, the EF_{N2O} is multiplied by various N inputs from the synthetic N fertilizers added, organic N sources applied (e.g., manure, compost, sewage), and residue N returned. Regarding the residue N returning to soils, only two default EF_{N2O} values for wet and dry climates (i.e., 0.6% and 0.5%, with an uncertainty range of 0.0%–1.1%) are considered when estimating N_2O emissions (IPCC, 2019b). Moreover, the EF_{N2O} value only considers the amount and N content of crop residues, while neglecting the potential importance of its chemical composition and moisture content. Significant N_2O emissions following the input of crop residues with a low C/N ratio (≤15) have been documented; meanwhile, the incorporation of residues with a high C/N ratio (>40) produced insignificant changes or even reduced soil N_2O emissions (Akiyama et al., 2020; Li et al., 2020; Pugesgaard et al., 2017). Specifically, the composition of organic N and C compounds in the soluble, cellulose, and lignin-like fractions determine the N mineralization potential of residues, and this affects the fate of the incorporated residue N, as it may be immobilized in soil fractions or lost to the environment through the gaseous and hydrological pathways (Lashermes et al., 2010). The composition of easily and slowly mineralizable organic matter significantly differs among various residues, and fresh green materials are generally decomposed faster than straw (Schmatz et al., 2017). Therefore, and not surprisingly, a meta-analysis of the existing literature by Chen et al. (2013) revealed that the EF_{N2O} of crop residues varies widely, with cereal and legume residues presenting lower values than vegetable residues. However, the effects of the composition of crop residues and the resulting interactions among mineralization, N dynamics, and N trace gas emissions have rarely been explored, and most relevant studies have characterized residues based solely on their N content or C:N ratio.

While the effects of residue incorporation on soil N_2O emissions have been extensively studied, its effects on soil NO emissions have been rarely examined. Typically, NO and N_2O are interrelated in the soil N cycling processes. Therefore, estimating the combined emissions of residue-induced NO and N_2O ($NO+N_2O$) across different residue types would provide insight into their integrative role in biogeochemistry. Contrary to that for soil N_2O emissions, nitrification, rather than denitrification, has been identified as the most important process driving soil NO emissions (Medinets et al., 2015). In a meta-analysis of nine studies, Liu et al.

(2017) reported that crop residue incorporation significantly decreased soil NO emissions. Similar to the observations for N_2O, the NO residue quality affects the magnitude of emission. Akiyama et al. (2020) reported the annual EF_{NO} value of 1.35%–2.44% and 0% for the crop residues of potato and cabbage. Meanwhile, Liu et al. (2011) reported the EF_{NO} value of 0.42% for wheat straw residues. However, there is paucity of research addressing NO losses following management using different types of crop residues.

Furthermore, residue decomposition in soils results in the volatilization of ammonia (NH_3), which is a precursor of secondary aerosols, leading to haze pollution (Liu et al., 2019) as well as soil acidification (Rennenberg and Gessler, 1999; Van Der Eerden et al., 1998) and eutrophication (Bobbink et al., 1992) NH_3 production and volatilization are the physiochemical processes that are mainly controlled by temperature and soil pH. They are directly linked to the decomposition of organic matter and release of NH_4^+, which remains in equilibrium with gaseous NH_3 depending on soil pH (Francis et al., 2008). Nett et al. (2016) found that 0%–1.6% of residue N was emitted as NH_3 following the incorporation of cauliflower residues in fields with different soil types. In addition, Xia et al. (2018) reviewed the potential of increased NH_3 volatilization following straw residue return and concluded that residue N volatilization in the form of NH_3 can mainly be attributed to the stimulation of soil nitrification/ denitrification and urease activity. However, little is known regarding the possible effects of the chemical composition of different residue types on NH_3 volatilization loss.

To this end, the objective of the present study was to investigate the effects of the incorporation of different crop residue types on the soil emissions of N_2O, NO, and NH_3 under standardized soil environmental conditions and to explore the link between the observed differences in the magnitude of N trace gas emission with residue properties, including soluble, cellulose, and lignin-like fractions. Briefly, the chemical composition of nine crop residues varying in terms of plant species and agricultural use was characterized according to different chemical criteria affecting decomposition dynamics, and the residues were evaluated for their potential to stimulate N trace gas emissions. Since the short-term responses of N trace gas emissions are expected following residue incorporation into soil, an automated mesocosm system allowing for 3-hourly flux measurements was used. Moreover, to link the microbial activity to N turnover processes and reactive N emissions, CO_2 fluxes and soil mineral N (NO_3^- and NH_4^+) concentrations were monitored throughout the incubation period. We hypothesized that in addition to the total N content or C/N ratio of the residue, the magnitude of and variations in soil N_2O, NO, and NH_3 emissions significantly depend on the other biochemical characteristics of the residue, such as soluble, cellulose, and lignin-like fractions. Furthermore, we hypothesized that following residue incorporation, N_2O emissions are greater than NO emissions and that the N_2O-to-NO emission ratio is modulated by the composition of the cytoplasmic compounds of residue cells (soluble) and cell-wall compounds (hemicellulose, cellulose, and lignin-like fractions), as these may control the stimulating effects of residues on soil microbial activity and O_2 consumption.

2. Materials and methods

2.1. Experimental design and soil and crop properties

The experiments were conducted at the laboratory facilities of IMK-IFU, KIT, Garmisch-Partenkirchen, Germany. Topsoil (0–20 cm) was

sampled from an arable site near Gießen, Germany (50°32′N, 8°41.3′E; 172 m. a.s.l.) in the summer of 2016. The soil samples were then homogenized, air-dried, and stored at 4 °C to limit further microbial activity during storage. The soil in this region is classified as Fluvic Gleysol with high organic matter and clay content (Appendix A, Table 1). Additional details are described by Malique et al. (2019). At the start of the 60-day experiment, the air-dried soil samples were sieved to 6 mm, homogenized, and packed into cylinders (volume: 1520.1 cm^3). Briefly, the soil material was filled in layers of 2 cm and compressed to the bulk density of 1.3 g cm^{-3}, until reaching the final height of 8 cm (1317.4 g DW soil per core). For a pre-incubation period of 7 days, the WFPS of the air-dried soil samples was first reduced to 40%. The soil was removed by spraying the surface with deionized water multiple times to prevent surface overflow and allow homogeneous percolation throughout the depth of the soil column. The WFPS was controlled gravimetrically for soil water loss twice a week and, if necessary, soil moisture was readjusted by spraying the soil with deionized water. The incubation temperature was maintained at 15 °C. After the 7-day pre-incubation period, crop residue material (5.1 g DW per soil core, equivalent to 4 t DM ha^{-1}) was incorporated manually into the topmost soil layer (4 cm), and the soil was subsequently recompressed to the bulk density of 1.3 g cm^{-3}. In the control treatment, crop residue material was not incorporated, but tillage was simulated, which resulted in the mixing of the soil until the depth of 4 cm. This allowed us to distinguish the effects of residue incorporation from those of soil disturbance and aeration on trace gas emissions. Following residue incorporation (day 0), the soil moisture was adjusted to the target value of 60% WFPS. Overall, two sets of soil cores were used and treated identically. One set ($n = 3$ soil cores per treatment) was used for the measurement of N$_2$O, NO, NH$_3$, and CO$_2$ fluxes using an automated soil incubation system (Section 2.2) and the other ($n = 4$ soil cores per treatment) was used for destructive sampling to determine soil mineral N concentrations (Section 2.6).

The aboveground plant material of nine crops was selected for the experiment: ryegrass (Ry), winter wheat (WW), oilseed rape (OS), field pea (PAE), maize (Ma), potato (Po), red clover (RC), mustard (Mu), and sugar beet (SUB). The effects of the incorporation of these residues in soil were compared with those of the control treatment (CO), in which crop residues were not incorporated (Appendix A, Table 2). The different plant parts (leaves and stems, among others) were hand-cut into pieces of 1 cm and mixed in proportions similar to their occurrence in the field. RC, Ma, and Ry materials were obtained from the field experimental site at the Norwegian University of Life Sciences in Ås, Norway and the remaining materials were obtained from the experimental site at the INRAE in Estrées-Mons in July 2017. After harvesting, the plant material was dried at 35 °C under ventilation to prevent further ripening, and the residual humidity was determined by drying the samples at 80 °C. Depending on the crop residue type and maturity stage during harvest, the plant material was rehydrated to two pre-defined water content levels (80% or 20%) before incorporation; these values are typical for residues either incorporated at the green stage during their vegetative growth and physiological maturity or at the senescent stage following full ripening, respectively (Appendix A, Table 2). Using ground material (80 μm), the biochemical characteristics of each residue type were determined in triplicate in the laboratories at the INRAE. Specifically, the total C and N content was determined using elemental analysis (NA2000, Fisons Instruments, Milan, Italy). The water-soluble organic C (SWC) and dissolved N (SWN) content of the residue was determined by aqueous extraction (30 min, 20 °C). The SWC content of the aqueous extract was quantified using an autoanalyzer (1010, O.I. Analytical Aurora Model 1030), and the SWN content was determined through dry combustion according to the standard NF EN 12260 (AFNOR, 2004). The N-NH$_4^+$ and N-NO$_3^-$ content was measured using continuous-flow colorimetry. Then, the chemical composition was determined using two-step proximate analysis (Goering and Van Soest, 1970). In the first step, the soluble compounds (SOL-

VS) were extracted from 1 mm ground plant material in hot water (30 min, 100 °C) and then in neutral detergent (1 h, 100 °C). In the second step, concentrated H$_2$SO$_4$ (72%) was used for the selective extraction of acid detergent fiber (ADF) material, and the final mass of the non-extractable material was considered acid detergent lignin (ADL). Ash content was measured at 550 °C for 4 h. The resulting extracts were then successively subtracted to determine the hemicellulose (HEM = NDF-ADF), cellulose (CEL = ADF-ADL), and lignin (LIG = ADL + ash) fractions as the residual material, as described previously (Van Soest and McQueen, 1973).

2.2. Automated soil incubation system for soil N and C trace gas flux measurements

The automated soil incubation system (Fig. 1) allows for the continuous and unattended monitoring of soil–atmosphere trace gas exchange under controlled laboratory conditions. It encompasses a set of 18 soil cores (inner diameter: 127 mm; height, 120 mm; polymethylmethacrylate material; SAHLBERG GmbH & Co. KG, Germany), which are distributed among two thermostatic incubation cabinets for temperature control at 15 °C (Lovibond ET 651-8, Tintometer GmbH, Dortmund, Germany). A pressurized ambient air storage tank continuously supplies air to the soil mesocosm system for an entire measuring cycle of 180 min. As the humidity of the air coming from the pressure tank was low, it was removed with deionized water to a relative humidity of 80% (RH/T probe HC2-S3C03, ROTRONIC Messgeräte GmbH, Germany). The headspace air exchange for each soil core was adjusted to 400 mL min^{-1} using mass flow controllers (MFCs; Bronkhorst High-Tech B.V.) (Fig. 1). In general, the air from the outlet of the soil cores is directed toward acid traps to capture NH$_3$ in the air stream and, for short 6 min periods, it is redirected toward gas analyzers to measure NO, N$_2$O, CH$_4$, and CO$_2$ concentration. During this 6 min period, the sample air is first dried with a permeation dryer (PermaPure Inc., Lakewood, USA) before being fed to the gas analyzers (Fig. 1). The flow rate to the gas analyzer, the overflow that was not used for analysis, and the flow rate of the pre-analyzer tube were recorded using mass flow meters (MFMs) (Fig. 1). The measurements of trace gas concentrations in the ambient background air (inlet) and in the headspace air originating from the individual soil mesocosms as well as periodic measurements of the calibration gas were performed automatically following a defined sampling sequence. The sequence involved continuous repetition of a 180-min cycle, in which each soil core was sampled once for 6 min, with alternate measurements of gas concentrations in the ambient background air (inlet) and calibration gas.

2.3. Measurements of N$_2$O, CO$_2$, and NO concentrations and fluxes in the headspace air

The N$_2$O and CO$_2$ mixing ratios in the sample air stream were measured at 1 Hz using quantum cascade laser absorption spectroscopy (QCLAS, CW-QC-TILDAS Aerodyne Research Inc., MA, USA, acquired in 2008). The QCLAS instrument was calibrated every 2 weeks using two different sets of gas blends (N$_2$O: 357.8 and 839.7 ppb; CO$_2$: 452.6 ± 9.1 and 447.5 ± 9.1 ppm) in synthetic air (80% N$_2$ and 20% O$_2$). The NO concentration in the sample air was monitored using a chemiluminescence detector (CLD 88 p, Eco Physics AG, Duernten, Switzerland). The weekly calibration was performed and regulated via solenoid valves with NO standard gas (4.35 ppmv NO in synthetic air; Air Liquide GmbH, Germany) and synthetic air using a multigas calibration system (series 6100; Environics Inc., Tolland, CT, USA). To ensure that the trace gas concentrations were measured at the steady-state only, the mean gas concentration, as observed in the last 20 s of the 6 min measuring cycle per soil core were used for flux rate calculations. The flux rate was computed in a flow-through steady-state chamber (Butterbach-Bahl et al., 1997) by calculating the difference in trace gas concentration between an empty core (ambient air)

ARTICLE IN PRESS

B. Janz, F. Havermann, G. Lashermes et al.   Science of the Total Environment xxx (xxxx) xxx
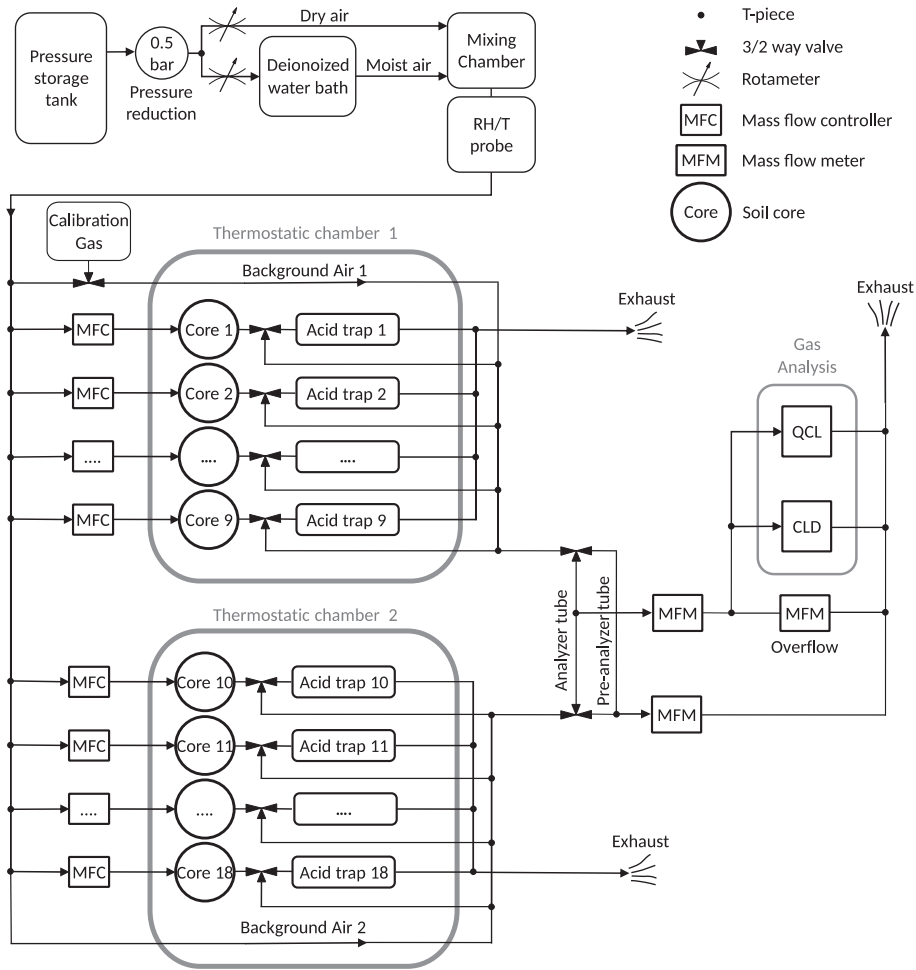
Fig. 1. Schematic overview of the automated soil incubation system for trace gas analysis of N_2O and CO_2 with quantum cascade laser absorption spectroscopy (QCLAS) as well as of NO with chemiluminescence detection (CLD) using 18 soil cores from varying crop residue treatments. Black lines represent the gas flow through 6 mm polytetrafluoroethylene tubes.

and soil-filled core (chamber air), considering the total air mass flow, using the following equation:

$$F_c = \frac{Q}{A} \times \rho(\mu_{cham} - \mu_{amb}) \qquad (1)$$

where F_c is the trace gas flux from the soil core (nmol m^{-2} h^{-1}); Q is the flow rate (m^3 s^{-1}); A is the surface area of the soil core; ρ is the molar density of the dry air molecules (mol m^{-3}), calculated based on the ideal gas equation; and μ_{amb} and μ_{cham} are the trace gas concentrations (nmol mol^{-1}) in the ambient and headspace air of the filled soil cores, respectively. During periods without measurements (e.g., manual sampling of NH_3 volatilization and refilling of soil water), all trace gas fluxes were linearly interpolated to obtain complete 3-hourly emission data as the basis for the calculation of cumulative emissions.

2.4. EFs

The EFs for N_2O (EF_{N2O}) and NO (EF_{NO}) were calculated as the cumulative additional effects of the treatments on gaseous N emissions (kg N ha^{-1}) relative to that of the control treatment, divided by the total N content of the plant residue (kg N ha^{-1}):

$$EF\ (\%) = \left[\frac{cum.N_{treatment} - cum.N_{control}}{residue\ N_{treatment}} \right] \times 100 \qquad (2)$$

2.5. Quantification of soil NH_3 volatilization

To quantify the rate of NH_3 volatilization, the outflowing headspace air was directed through individual acid traps to quantitatively capture NH_3 in the air stream. Each acid trap comprised a gas-washing bottle (ROBU VitraPOR Borosilicate Glass 3.3, Hattert, Germany) filled with 100 mL of a 0.1 mol L^{-1} oxalic acid ($C_2H_2O_4$) solution, which retained the NH_3 in the gas stream as dissolved NH_4^+. The gas inlet to the washing bottle was directed via a glass filter out of the borosilicate glass. The washing solution was replaced biweekly, and NH_4^+ concentration in the solution were determined colorimetrically using the indophenol method (Bolleter et al., 1961). Cumulative NH_3 volatilization was calculated based on the total amount of NH_4^+ captured during the incubation period.

2.6. Measurements of soil mineral N concentrations

Soil mineral N concentrations (NO_3^--N and NH_4^+-N) were measured at -5, 0, 4, 7, 14, 28, and 60 days after crop residue incorporation by sampling a set of soil cores that were only used for destructive sampling but otherwise treated in the same way as the soil cores used for gas flux measurements. Briefly, 10 g of soil was removed from the cores and extracted with 40 mL of 1 M KCl solution. The filtered extract was frozen until analysis at the Raiffeisen Laborservice (Raiffeisen Rhein-Ahr-Eifel Handelsgesellschaft mbH, Ormont, Germany). For the analysis, three subsamples were prepared from

both the upper soil column (0–4 cm) with the crop residue amendment and the lower soil column (4–8 cm) without the crop residue amendment. However, as no significant differences in soil organic N concentrations between the soil layers were noted, the data were pooled to calculate the mean soil inorganic N concentrations for individual sampling dates.

2.7. Statistical analyses

The collected data were analyzed using R (The R Foundation for Statistical Computing Platform, v3.6.3). The measured flux variables, except N_2O, passed the tests of normality and homoscedasticity. The N_2O fluxes were log-transformed and then analyzed. The significance of differences in cumulative N_2O, NO, NH_3, and CO_2 emissions among the crop residue treatments was determined by one-way analysis of variance (ANOVA). When the ANOVA indicated significant differences among treatments, Tukey's honestly significant different (HSD) post hoc test was performed at a probability level of 5% or lower using the

“agricolae” package in R. The correlation matrix (Appendix B, Fig. 3) of the biochemical parameters of the residues was constructed using the “corrplot” package in R. To overcome probable multi-collinearity among the predictor parameters, principal component analysis (PCA) and multiple regression analysis (MRA) with sequential predictor selection was performed. PCA was performed using the base R prcomp() function to explore the trends of associations of the gaseous N emissions and biochemical properties of residues. MRA with stepwise back and forward predictor selection (max $n = 5$) was performed using the “caret” package in R to identify models with the best subsets of residue biochemical parameters to predict cumulative emissions (i.e., N_2O, CO_2, NO, and NH_3), combined reactive N trace gas emissions (N_2O + NO and N_2O + NO + NH_3), and fractionation ratios (N_2O:NO, N_2O:CO_2, and N_2O:NH_3) based on the lowest model root mean square error (RMSE) as the selection criteria. For MRA, the soil core triplicates were considered independent flux measurement units, yielding 27 observations (9 crop residues × 3 replicates) that were used to identify the subset of coefficients and standardized beta coefficients with the highest
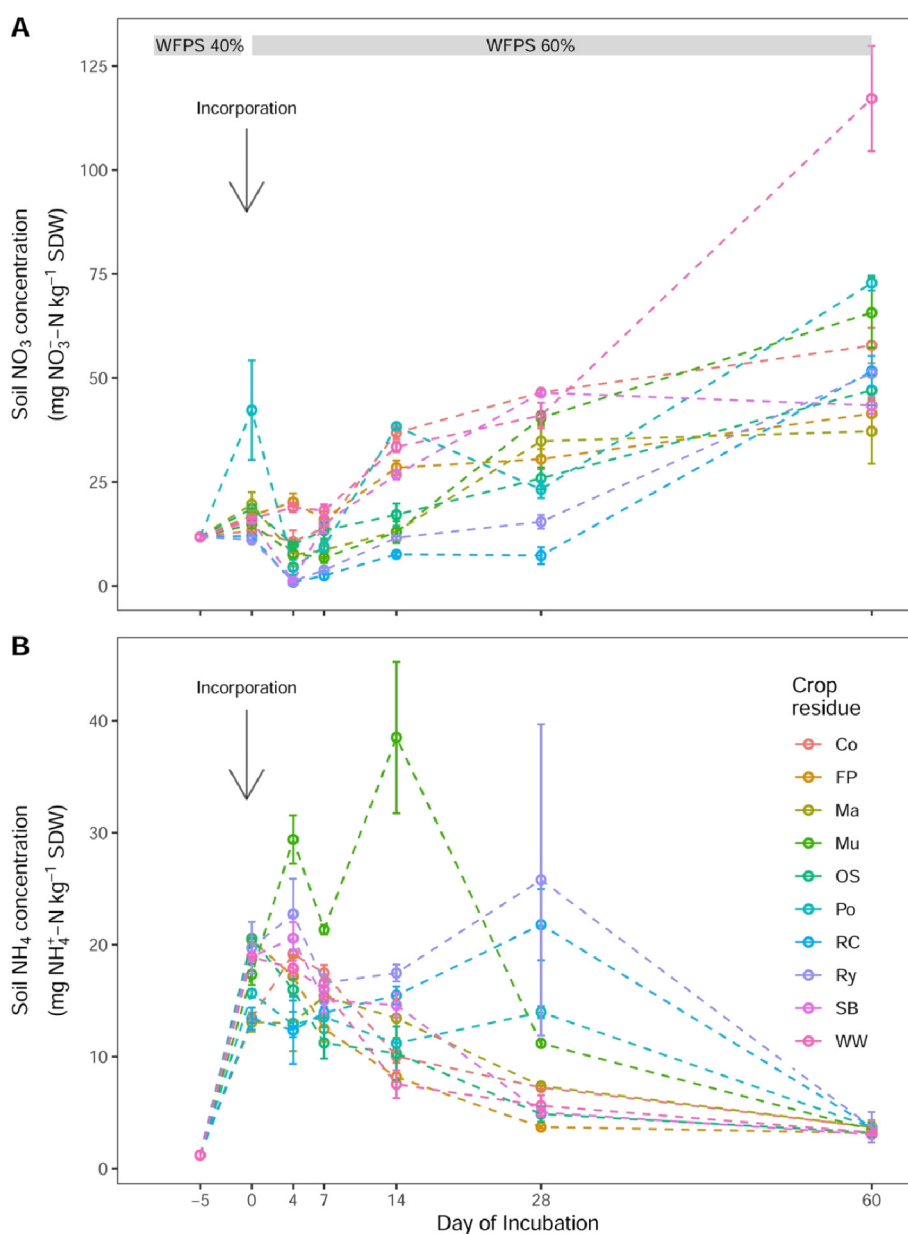
Fig. 2. Soil concentrations of nitrate (A) and ammonium (B) in the 0–8 cm soil layer (mean ± SE; $n = 3$) measured once before and six times during soil treatment with nine crop residues (FP: field pea; Ma: maize; Mu: mustard; OS: oilseed rape; Po: potato; RC: red clover; Ry: ryegrass; SB: sugar beet; WW: winter wheat) or control treatment (Co).

explanatory power. Data were expressed as the mean ± standard error (SE), and differences were considered significant at p < 0.05, unless specified otherwise.

3. Results

3.1. Effects of residue incorporation on soil mineral N concentration

The dynamics of soil mineral N (NO_3^- and NH_4^+) content are presented in Fig. 2. The average soil NO_3^- concentration 6 h after soil re-wetting and residue incorporation was 17.9 ± 1.0 mg N kg^{-1} soil dry weight (SDW). Under the control treatment (Co), the mean soil NO_3^- concentration was 13.8 ± 0.2 mg N kg^{-1} SDW, showing little change compared with the value in the dry soil before the start of the experiment (11.8 ± 0.6 mg N kg^{-1} SDW). The greatest increase in soil NO_3^- concentrations to the value of 43.9 ± 12.5 mg N kg^{-1} SDW was recorded following the incorporation of Po. The lowest soil NO_3^- concentration was recorded in most treatments 4 days after residue incorporation; thereafter, soil NO_3^- concentration increased steadily, reaching the maximum values in the range of 30–125 (mean: 63.2 ± 3.1) mg N kg^{-1} SDW 60 days after residue incorporation. At 60 days, the soil NO_3^- concentration under the control treatment was 60.1 ± 4.4 mg N kg^{-1} SDW.

At day 0, the mean NH_4^+ concentration in the re-wetted soil following residue incorporation was 17.5 ± 0.4 mg N kg^{-1} SDW, being slightly higher than the control value (13.9 ± 0.2 mg N kg^{-1} SDW) (Fig. 2). Under most residue treatments, the peak soil NH_4^+ concentration (for Mu: up to 40.1 ± 7.1 mg N kg^{-1} SDW) was reordered within the first 14 days following residue incorporation. Soil NH_4^+ concentrations declined toward the end of the experimental period (day 60) to values

<5 mg N kg^{-1} SDW, without significant differences among treatments or between the treatments and control.

3.2. Effects of crop residue incorporation on soil N$_2$O fluxes

Except under the Ry treatment, N_2O fluxes during the pre-incubation period were generally low (<7 µg N$_2$O-N m^{-2} h^{-1}) under most treatments. Crop residue incorporation in the 0–4 cm topsoil layer rapidly increased N_2O fluxes, peaking within the first 3 days, with the maximum values of up to ~6000 µg N$_2$O-N m^{-2} h^{-1} under the Mu and Ry treatments. Thereafter, within approximately 7 days, soil N_2O fluxes decreased to values below 50–100 µg N$_2$O-N m^{-2} h^{-1} (Fig. 3A). Under the Ry treatment, a second period of increase in N_2O fluxes (>100 µg N$_2$O-N m^{-2} h^{-1}) was noted, starting around day 7 and lasting for approximately 3 weeks.

Cumulative N_2O emissions significantly varied across the residue treatments (Figs. 3B and 4A), ranging from 0.34 ± 0.06 (FP) to 4.01 ± 0.39 kg N$_2$O-N ha^{-1} (Ry). In other words, cumulative N_2O emission from the crop residue-amended soil ranged from being 17% lower to six times higher than that from the unamended control soil (Co: 0.41 ± 0.11 kg N$_2$O-N ha^{-1}). Due to the wide variability in soil N_2O fluxes among the three replicates, significantly higher cumulative N_2O fluxes compared with the control value were only observed under the Ry, Mu, and Po treatments (Fig. 4A). However, the effects of residue incorporation were short-lived, and under most treatments, >80% of total N_2O emissions over the 60-day incubation period were observed during the first 2 weeks following residue incorporation (Fig. 3B).

The N content of the applied crop residues varied from 20 (WW and OS) to 134 (Po) kg N ha^{-1} (Fig. 4B; Appendix A, Table 2). Among all
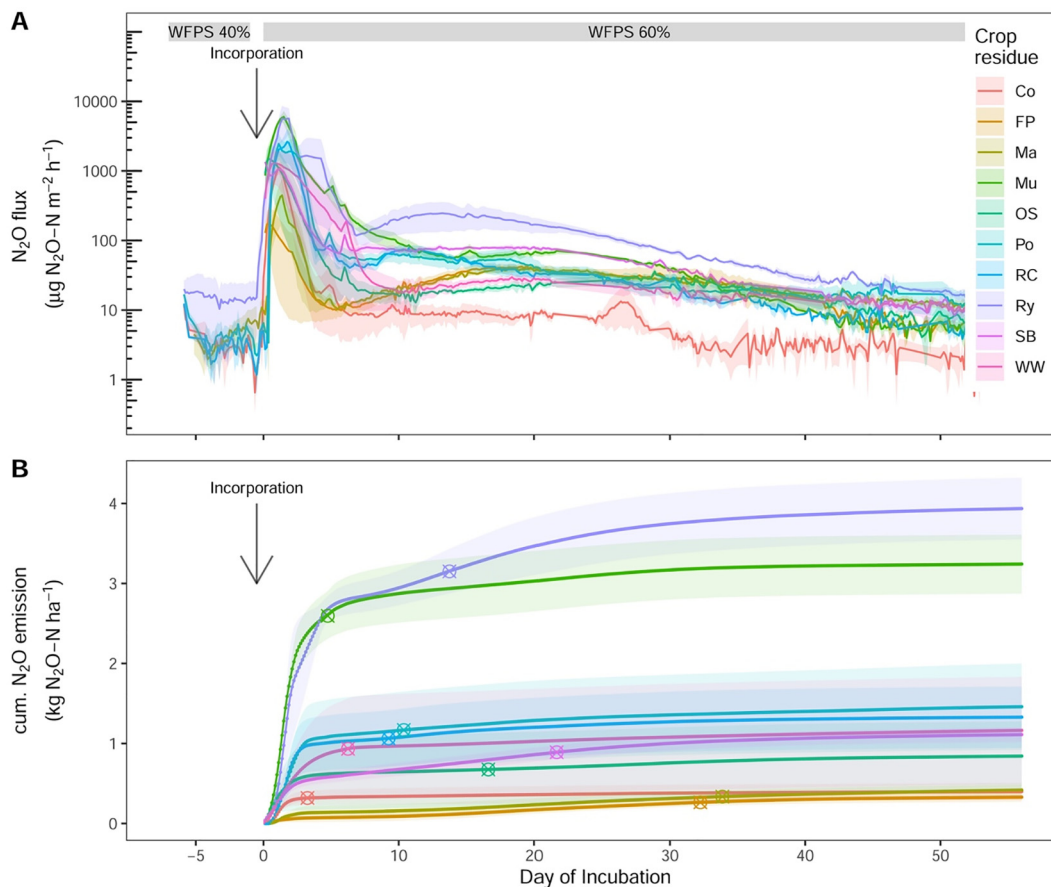
Fig. 3. Temporal changes in soil N$_2$O fluxes (mean ± SE; $n = 3$) in response to the incorporation of residues in the 4 cm topsoil layer over a 60-day incubation period. (A) Time series of fluxes under different treatments. (B) Cumulative N$_2$O fluxes. Arrows indicate the day of residue incorporation (4 t DW ha^{-1}). ⊗ in panel (B) indicates the time at which 80% of the total cumulative N$_2$O emission was reached. FP: field pea; Ma: maize; Mu: mustard; OS: oilseed rape; Po: potato; RC: red clover; Ry: ryegrass; SB: sugar beet; WW: winter wheat; Co: control.
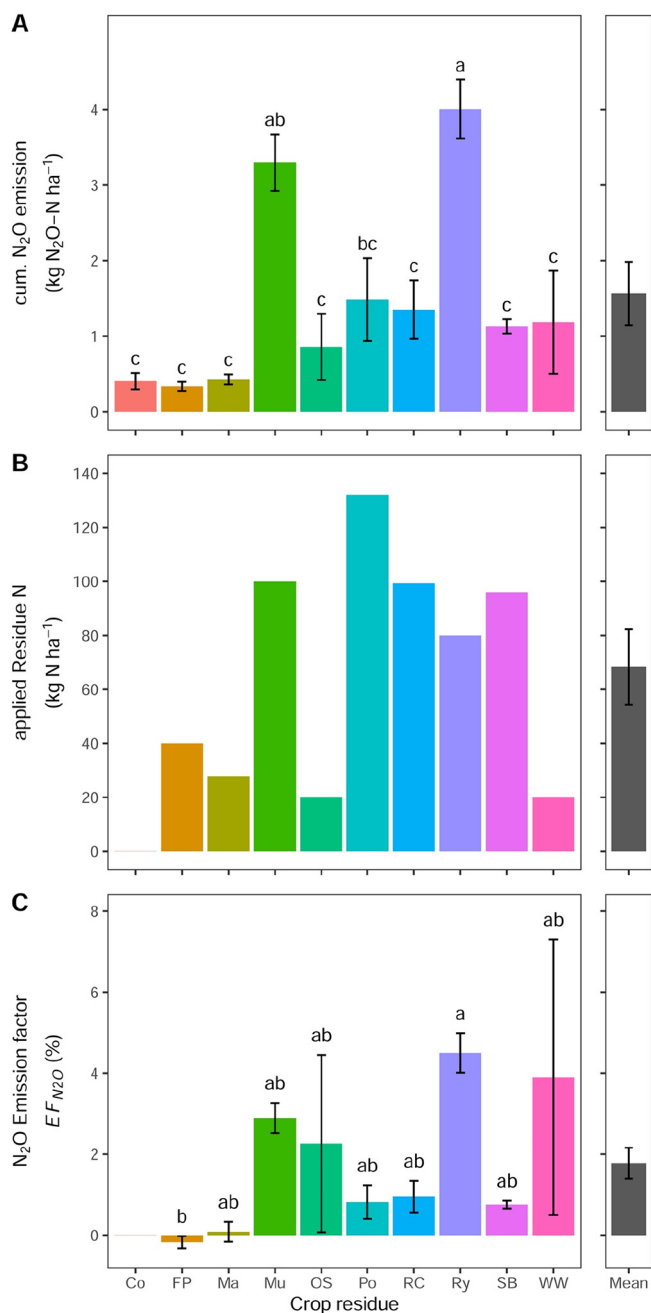
Fig. 4. Cumulative N$_2$O emission (mean ± SE; $n = 3$) from soil cores with or without residue incorporation (4 t DW ha^{-1}) over a 60-day incubation period (A). Total amount of residue N incorporated (B). Calculated residue N$_2$O emission factor (C). The same letters on bars indicate non-significant differences at $p = 0.05$. FP: field pea; Ma: maize; Mu: mustard; OS: oilseed rape; Po: potato; RC: red clover; Ry: ryegrass; SB: sugar beet; WW: winter wheat; Co: control. Overall mean ± SE ($n = 9$), excluding Co, is shown as the grey bar.

residue types, the mean EF_{N2O} for the incorporated residue N was 1.78 ± 0.38% (Fig. 4C), with the highest value recorded under the Ry treatment (4.5 ± 0.49%); conversely, the incorporation of FP residue reduced N$_2$O emissions, with a negative EF_{N2O} (−0.17 ± 0.15%) (Fig. 4C).

3.3. Effects of crop residue incorporation on soil NO fluxes

Contrary to N$_2$O fluxes, which increased immediately following residue incorporation, reaching peak emissions within the first 3 days, soil NO fluxes increased slowly under most treatments, except for Mu (Fig. 5). The peak NO emissions were recorded around day 20, with

values after residue incorporation being approximately 2–3 times higher than those during pre-incorporation period. However, NO fluxes returned to the background levels 40–50 days after residue incorporation (Fig. 5A). The highest soil NO fluxes and cumulative NO emissions (Fig. 5A, B) were recorded under the Ry treatment (0.41 ± 0.13 kg NO-N ha^{-1}). The cumulative emission under the control treatment was 0.07 ± 0.01 kg NO-N ha^{-1}. The overall mean NO emission following residue application was 0.23 ± 0.04 kg NO-N ha^{-1}.

The average NO EF (EF_{NO}) across all residue treatments was 0.34 ± 0.02% (Fig. 6B). The highest EF_{NO} was recorded under the OS (0.73 ± 0.08%) and WW (0.78 ± 0.07%) treatments, while the incorporation of Po and RC residues did not significantly affect soil NO emissions (EF_{NO} Po: 0.02 ± 0.01%; EF_{NO} RC: 0.005 ± 0.007%) (Fig. 6B).

3.4. Effects of crop residue incorporation on NH$_3$ volatilization

The total NH$_3$ volatilization rate over the 60-day experimental period following residue incorporation ranged from 2.2 to 5.4 kg N ha^{-1}, with the highest values recorded under the OS treatment (5.4 ± 1.2 kg NH$_3$-N ha^{-1}) and the lowest under the Ry treatment (1.6 ± 0.9 kg NH$_3$-N ha^{-1}). The rate under the control treatment was 2.4 ± 0.5 kg NH$_3$-N ha^{-1}. Overall, residue incorporation increased NH$_3$ volatilization by 25.1% (Appendix B, Fig. 1). However, due to the significant variability in fluxes among the replicates, no significant effect of residue incorporation was observed on NH$_3$ volatilization.

3.5. Effects of crop residue incorporation on soil CO$_2$ fluxes

The temporal dynamics of soil CO$_2$ fluxes over the 60-day incubation period are presented in Appendix B, Fig. 2. The CO$_2$ flux immediately increased after residue incorporation, with the maximum values of soil respiration recorded under the RC treatment (629 ± 202 mg CO$_2$-C m^{-2} h^{-1}). After the first 1–2 days, soil respiration declined exponentially until the end of the experiment, with short-lived spikes of emissions due to the re-adjustment of soil moisture (days 5/6, 28; Appendix B, Fig. 2A). The cumulative soil CO$_2$ emission from the unamended soil (Co: 435 ± 131 kg CO$_2$-C ha^{-1}) was significantly lower than that from the crop residue-amended soil, with the highest value recorded under the Ry treatment (Appendix B, Fig. 2B). There were no significant differences in the cumulative CO$_2$ emission across the plant residue treatments throughout the incubation period.

3.6. Effect of the biochemical parameters of residue on soil N trace gas fluxes and respiration

To explore the trends of relationships of the biochemical properties and maturity stage of residue with soil N trace gas emissions and respiration, PCA was used. The first principal component (PC1) separated the residues with high SOL-VS, SWC, and N on the right and those with high C/N ratio and CEL on the left. The second principal component (PC2) separated the residues with high HEM (specifically Ry) at the top and those with high NO$_3^-$ (in particular Po residues) at the bottom. NO and NH$_3$ emission were not well projected in this plane. Meanwhile, N$_2$O and CO$_2$ emissions were strongly and positively correlated with each other and with the residue maturity stage (green) but negatively correlated with LIG.

Stepwise MRA was used to further explore the relationships of the N$_2$O, NO, NH$_3$, CO$_2$ emissions with the biochemical components of crop residues. As shown in Table 1, the SWC and LIG fractions of the residue had a significant but negative effect on N$_2$O emission, while SOL-VS had a significant and positive effect. The NO$_3^-$ content and CEL fraction of the residue, though not significantly, further explained the variability in N$_2$O emission, with an overall coefficient of determination (R^2) of 0.776. The variability in cumulative NO emissions due to residue incorporation was best explained ($R^2 = 0.515$) by the SOL-VS fraction (positive effect) as well as the N content, SWC content, and CEL fraction
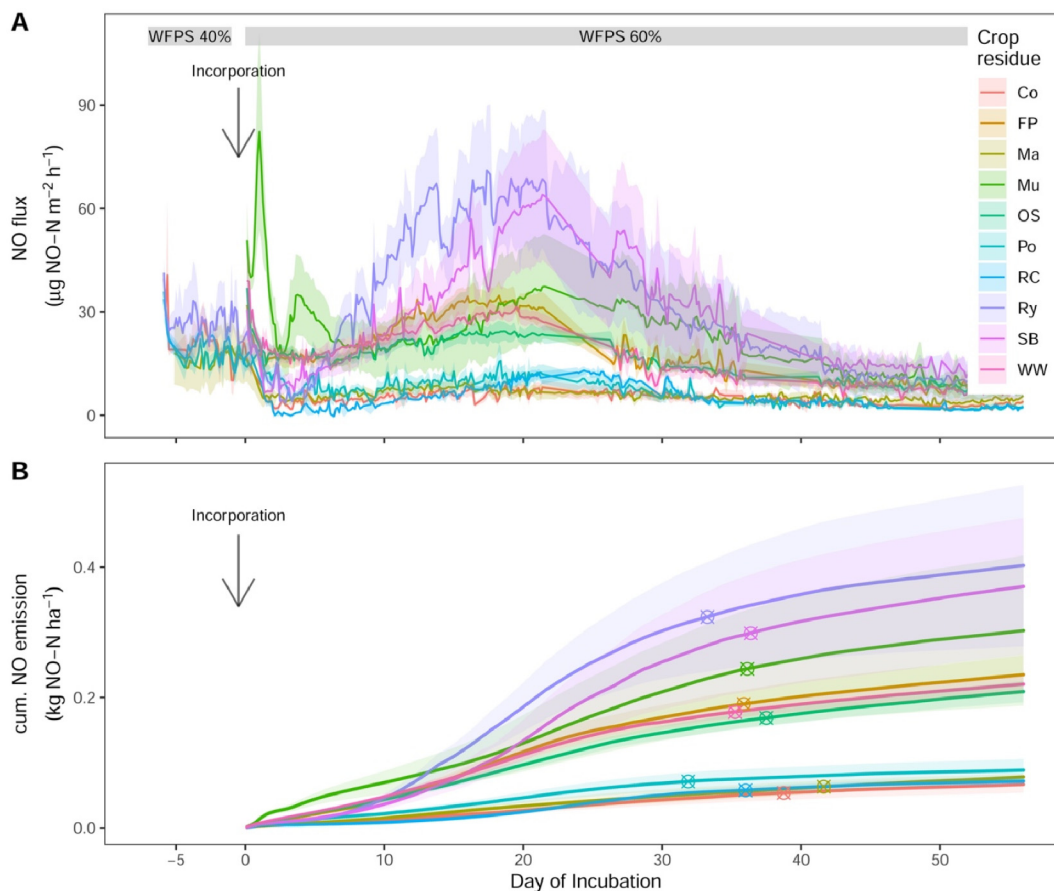
Fig. 5. Temporal changes in soil NO fluxes (mean $\pm$ SE; $n = 3$) in response to the incorporation of residues in the 4 cm topsoil layer over a 60-day incubation period. (A) Time series of fluxes under different treatments. (B) Cumulative NO fluxes. Arrows indicate the day of residue incorporation (4 t DW ha^{-1}). $\otimes$ in panel (B) indicates the time at which 80% of the total cumulative NO emission was reached. FP: field pea; Ma: maize; Mu: mustard; OS: oilseed rape; Po: potato; RC: red clover; Ry: ryegrass; SB: sugar beet; WW: winter wheat; Co; control.

(negative effect) of the residue. The magnitude of cumulative soil NH_3 volatilization was mainly dependent on the NH_4^+ content of the residue, although the overall explanatory power of the relationship remained low ($R^2 = 0.2$). The variability in cumulative soil respiration among treatments was best explained ($R^2 = 0.866$) the NO_3^- content (negative) as well as the total N and NH_4^+ content and the CEL and HEM fractions of the residue.

The residue maturity stage was not included as a variable in the initial MRA (Table 1) because our experimental design only described two stages (i.e., green vs. senescent). When included as a categorical variable in MRA (Table 2), the green stage was proven the key variable for predicting N_2O and NO emissions and soil respiration (CO_2).

4. Discussion

4.1. Residue N content or C/N ratio alone cannot explain the variability in soil N_2O emissions

In the present study, 1.79% of the incorporated residue N was emitted in the form of N_2O. However, the mean value did not reflect the wide variability in EF_{N2O} observed; as such, the EF_{N2O} values of the incorporated crop residue varied from -0.17 to 4.5% (Fig. 4C). Since the residue application rate was constant at 4 t DW ha^{-1}, the observed variability in EF_{N2O} may be related to the N content of the incorporated residue, which also showed a wide range (20–134 kg N ha^{-1}) (Fig. 4B). However, the highest EF_{N2O} value was recorded for WW and OS (both 20 kg N ha^{-1}), which showed the lowest N content. Thus, parameters other than N content must play a role in controlling N_2O emissions and warrant consideration in the estimation of EF_{N2O} for crop residues.

Diverse residue types reportedly affect the magnitude of soil N_2O emission, and the high rate of soil N_2O emission is affected by the C/N ratio of the applied residues (Baggs et al., 2000; Huang et al., 2004). Specifically, the C/N ratio of ~30 is widely accepted as the critical value (Chen et al., 2013). Accordingly, the incorporation of residues with a C/N ratio of <30 is expected to promote soil N availability and N_2O emission; conversely, following the incorporation of residues with a C/N ratios exceeding 30, soil N may be immobilized, while N_2O emissions may remain unaffected or even diminish. The present study also provides evidence for the critical C/N threshold of ~30. In the present study, the incorporation of some residues with C/N ratios exceeding 30 showed similar (Ma: C/N = 66) or reduced (Fp: C/N = 43) N_2O emissions compared with the control treatment (Fig. 3A; Appendix B, Fig. 4). However, the incorporation of WW or OS residues with a C/N ratio of ~100 increased soil N_2O emissions compared with the control treatment (Fig. 3A; Appendix B, Fig. 4). Similar observations have been reported by Li et al. (2013) for crop residues with a C/N ratio exceeding 100, suggesting that this attribute is not a reliable predictor of the potential of crop residue to stimulate soil N_2O emission. The inconsistent responses of soil N_2O emissions to the incorporation of crop residues with a high C/N ratio may be explained based on work of Kravchenko et al. (2017), who showed that the incorporation of residues with a high C/N ratio stimulated heterotrophic microbial activity, which may lead to a depletion of O_2 concentration and thereby increasing the likelihood of soil anaerobicity and N_2O production hotspot formation.

In contrast, in the present study, the incorporation of residues with C/N ratios below 25 (i.e., SB: 16, Po: 12, RC: 18, Mu: 16, and Ry: 23) (Fig. 3A; Appendix B, Fig. 4) resulted 2–3 times higher soil N_2O
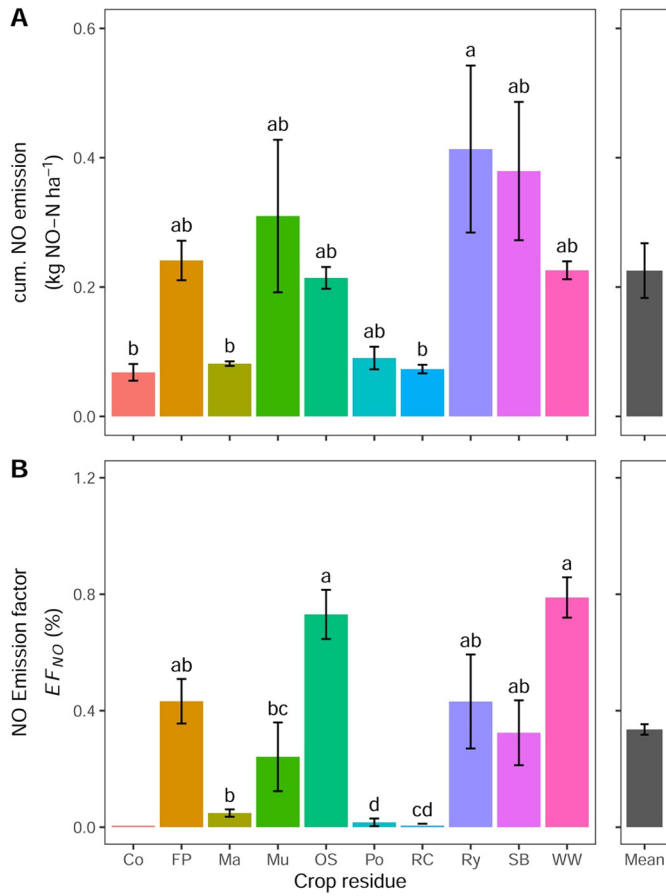
Fig. 6. Cumulative NO emissions (mean ± SE; $n = 3$) from soil cores with or without residue incorporation (4 t DW ha^{-1}) over a 60-day incubation period (A). Calculated residue NO emission factor (B). The same letters on bars indicate non-significant differences at $p = 0.05$. FP: field pea; Ma: maize; Mu: mustard; OS: oilseed rape; Po: potato; RC: red clover; Ry: ryegrass; SB: sugar beet; WW: winter wheat; Co: control. Overall mean ± SE ($n = 9$), excluding Co, is shown as the grey bar.

emissions than the control treatment. However, given the significant variability in soil N_2O emissions in response to the incorporation of residues with a wide range of C/N ratios in our experiment as well as in a meta-analysis by Charles et al. (2017), the biochemical composition and other soil factors evidently play a role in determining the N_2O emission potential of crop residues.

4.2. Biochemical composition of the residue affects N_2O emission

Depending on the crop type, the biochemical composition of the residues may vary significantly in terms of the concentration of lignin (LIG), cellulose (CEL), hemicellulose (HEM), and sugars (SOL-VS) (e.g., Kriaučiuniene et al., 2012). These compounds present specific decomposition rates. For instance, the decomposition of LIG is slower, requiring months to years, than that of other soluble low-weight compounds, which are decomposed within days to months (Devêvre and Horwáth, 2000; Vanlauwe et al., 1996). Our PCA revealed the distinct separation of residues with a higher fraction of soluble compounds (SOL-VS and SWC) and those with a higher fraction of structural compounds (CEL or LIG). Furthermore, our stepwise MRA considering the biochemical characteristics of residues showed that the SWC content and the SOL-VS and LIG fractions are the key predictors of the potential of crop residue to stimulate soil N_2O emission (highly significant, $p < 0.001$; Table 1). In addition, a greater proportion of structural fractions, such as insoluble LIG, in the residue (e.g., WW and FP) would reduce soil N_2O emissions, possibly due to increased N immobilization (Yansheng et al., 2020). As such, when microorganisms

Table 1
Results of multiple stepwise linear regression analyses of the fluxes of N trace gas, parameters of soil respiration, and biochemical properties of incorporated residues. Stepwise regression coefficients with associated p levels, standardized beta coefficients, and coefficients of determination (R^2/R^2 adjusted) are shown for each selected model (27 observations). NO_3: residue NO_3^- concentration, SWC: water-soluble C, SOL-VS: neutral detergent soluble fraction, CEL: cellulose fraction, HEM: hemicellulose fraction, LIG: lignin + ash fraction, N: total N content, NH_4: residue NH_4^+ concentration, C/N: residue C/N ratio.

Predictors	N_2O Estimates	N_2O Beta	NO Estimates	NO Beta	NH_3 Estimates	NH_3 Beta	CO_2 Estimates	CO_2 Beta	N_2O+NO Estimates	N_2O+NO Beta	$N_2O+NO+NH_3$ Estimates	$N_2O+NO+NH_3$ Beta	$N_2O{:}NO$ Estimates	$N_2O{:}NO$ Beta	$N_2O{:}CO_2$ Estimates	$N_2O{:}CO_2$ Beta	$N_2O{:}NH_3$ Estimates	$N_2O{:}NH_3$ Beta
(Intercept)	−0.65		0.74		−3.03		−2996.51**		4.79***		−42.25*		4206.48		0.00*		2.00*	
NO3	1.12	0.22					−1539.78***	−1.59	−6.91***	−1.22			−43,235.34*	−0.59	−0.00***	−2.27		−0.29
SWC	−1.08***	−2.45	−0.13**	−2.50					−1.83***	−3.97	−0.42	−0.68	−155.56	−0.03				
SOL-VS	0.22***	2.80	−0.02***	2.54	0.06	0.50	51.97***	2.75			0.48**	4.40	−125.91	−0.12	0.00**	2.06		
CEL	0.11	1.06	−0.01	−1.00							0.59*	3.91						
LIG	−0.36**	−1.26	−0.15*	−0.95					−0.31***	−1.04								
N							864.13***	3.72	4.35***	3.18					−0.00*	−0.64		−0.10
NH4					67.31*	0.62	8915.45*	0.56	112.82***	1.20	106.29*	0.84	182,241.50	0.15				
HEM							27.61**	0.84			0.37*	1.40						
C/N													−34.79	−0.06				
R^2/R^2adjusted	0.776/0.723		0.515/0.427		0.200/0.134		0.866/0.835		0.839/0.801		0.401/0.258		0.308/0.143		0.483/0.415		0.083/0.046	

* $p < 0.05$.
** $p < 0.01$.
*** $p < 0.001$.

ARTICLE IN PRESS

B. Janz, F. Havermann, G. Lashermes et al.   Science of the Total Environment xxx (xxxx) xxx

Table 2
Results of multiple stepwise linear regression analyses including residue maturity stage. N trace gas fluxes and soil respiration parameters explained by variables characterizing the biochemical properties of the incorporated residues are shown. Stepwise regression coefficients with associated p levels, standardized beta coefficients, and coefficients of determination (R^2/R^2 adjusted) are shown for each selected model (27 observations). NO_3: residue NO_3^- concentration, SWC: water-soluble C; SOL-VS: neutral detergent soluble fraction; CEL: cellulose fraction; HEM: hemicellulose fraction; LIG: lignin + ash fraction, N: total N content, NH_4: residue NH_4^+ concentration, C/N: residue C/N ratio.

Predictors	N2O Estimates	N2O Beta	NO Estimates	NO Beta	NH3 Estimates	NH3 Beta	CO2 Estimates	CO2 Beta	N2O + NO Estimates	N2O + NO Beta	N2O + NO + NH3 Estimates	N2O + NO + NH3 Beta	N2O:NO Estimates	N2O:NO Beta	N2O:CO2 Estimates	N2O:CO2 Beta	N2O:NH3 Estimates	N2O:NH3 Beta
(Intercept)	9.86**	−1.13	0.17*	−0.84	3.03	0	−1377.1***	−1.17	9.04**	−1.27	2.92**	−0.36	4206.478	0	0.00*	0	2.00*	0
Maturity [green]	3.38***	2.53	0.30**	1.90			623.74***	2.63	3.98***	2.85	1.15*	0.80						
SWN	7.72***	1.10							8.36***	1.14								
SWC	−1.14***	−2.58	−0.06**	−1.14					−1.18***	−2.55			−155.56	−0.03	−0.00***	−2.27		
HEM	−0.11*	−0.58							−0.09*	−0.49	−0.08	−0.29						
LIG	0.38**	−1.32							−0.33*	−1.12								
C/N							12.12**	0.37					−34.79	−0.06	−0.00*	−0.64	−0.10	−0.29
NH4			6.63*	0.62	67.31*	0.62							182,241.50	0.15				
CEL					0.06	0.50												
N							33.55***	1.78										
NO3							332.18***	1.43					−43,235.34*	−0.59				
SOL-VS													−125.91	−12.00	0.00**	2.06		
R^2/R^2adjusted	0.813/0.769		0.403/0.325		0.200/0.134		0.883/0.861		0.838/0.800		0.231/0.167		0.308/0.143		0.483/0.415		0.083/0.046	

* $p < 0.05$.
** $p < 0.01$.
*** $p < 0.001$.

decompose crop residue as a source of energy and C to support their growth and reproduction, they require N to build cellular components (Robertson and Groffman, 2015), which limits substrate availability for nitrification and denitrification.

The stimulating effect of residues with a high SOL-VS fraction on soil N_2O emissions was likely associated with the promotion of microbial activity due to the enhanced sugar, starch, and protein availability. Increased microbial activity supports the formation of anoxic hotspots in or around the moist residue particles in soil, thus creating soil environmental conditions conducive to high denitrification activity and N_2O production (Kravchenko et al., 2017). Our measurements of soil respiration (Appendix B, Fig. 2) support this hypothesis: following the incorporation of residues with high SOL-VS concentrations (RC, SB, Mu, Po, and Ry), soil CO_2 fluxes were increased greatly, whereas following the incorporation of residues with low SOL-VS concentrations (FP, Ma, OS, and WW), the stimulation of soil respiration was distinctly lower. Moreover, the rapid reduction in soil NO_3^- concentration following the incorporation of crop residues implies a high rate of denitrification and, simultaneously, a low rate of nitrification in the first 4 days after the amendment (Fig. 2A). This assumption was supported by the observed increase in the soil NH_4^+ concentration during the same period (Fig. 2B).

The SOL-VS fraction and SWC content were strongly and positively correlated, as demonstrated by the narrow projection of the two variables in the PCA biplot (Fig. 7). Although our MRA results suggested a negative relationship between the SWC content and N_2O emission (Table 1), SWC in decomposing plant material has been reported to support the formation of anoxic microsites and denitrification in agricultural soils (Surey et al., 2020). The abundance of readily available dissolved C substrates relative to the soil available N promotes denitrification and increases the N_2O-to-N_2 ratio (e.g., Ingwersen et al., 1999). According to Ingwersen et al. (1999), if the availability of SWC relative to that of soil N is high, denitrifiers may express the complete denitrification enzyme chain, such that N_2 becomes the sole end product of denitrification. This mechanism may explain the observed high N_2O emissions following the incorporation of the WW and OS residues, which presented the highest C/N ratios but the lowest SWC content, in the present study. Under these conditions, the anaerobic hotspot created by the incorporation of residues (Kravchenko et al., 2017) may be carbon- rather than nitrogen-limited, resulting in increased N_2O production during denitrification.

The PCA biplot (Fig. 7) revealed a strong and positive correlation between the residue stage maturity and the CO_2, N_2O, and NO emissions. The residue maturity stage was not included as a variable in stepwise selection in the initial MRA (Table 1), because our experimental design only described two stages (green vs. senescent), which do not reflect the entire spectrum of real-world conditions. Nevertheless, when included as a categorical variable, the residue maturity was selected as the key predictor of CO_2, NO, and N_2O emissions (Table 2). Thus, the incorporation of green residues with a moisture content of 80% significantly stimulated microbial activity compared with the incorporation of senescent residues with a moisture content of 20%. The inclusion of maturity as a variable removed the SOL-VS fraction from the best subset model and promoted the SWN and SWC content of the residue to become the significant predictors of N_2O emission. Overall, our experiment indicated that residue maturity may be used as a simple and effective method for classification and, thus, as a proxy for the biochemical characteristics of residues. However, the strong relationship between maturity stage and N_2O emission warrants further screening of crop residues with a wider range of moisture levels under standardized conditions of oxygen supply—representative of the field conditions.

4.3. Review of the IPCC EF_{N2O} values for different crop residues

Most of the current national emission inventory methods use direct EF_{N2O} with a single default value of 1% for N input from organic
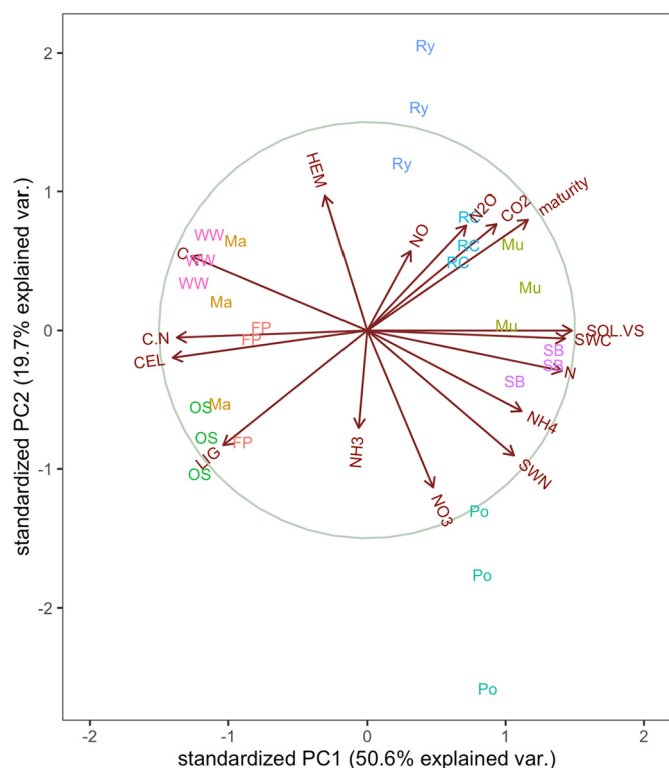
Fig. 7. Projection of the chemical components of the residue and the emissions of N_2O, NO, NH_3, and CO_2 following the incorporation of nine types of residues. Observations on the plane defined by the first two components of principal component analysis (PCA) are presented. The variables are represented by arrows. The coordinates of each variable indicate the correlation coefficients on the first two principal components. The variables are better represented in the plane when the arrow points are close to the circle. When they are correctly represented, the correlations between parameters are stronger and the angle between their directions is smaller. The first and second axes of PCA explained 70% of the total variance. C: carbon content; CEL: cellulose; HEM: hemicellulose; LIG: lignin and ash; N: nitrogen; C:N: C/N ratio; SWN: water-soluble N; SWC: water-soluble C; SOL-VS: natural detergent fiber extract; NO_3: nitrate; NH_4: ammonium; maturity: senescent vs green stage of residue at incorporation; N_2O: cumulative N_2O emission; NO: cumulative NO emission; NH3: cumulative NH_3 emission; CO_2: cumulative CO_2 emission.

amendments (IPCC, 2006). In 2019, the IPCC revised the residue EF_{N2O} and suggested differentiating the effects of residue N on soil N_2O emissions in dependence of climate. The currently recommended values of the residue N EF_{N2O} are 0.6% (0.1–1.1%) and 0.5% (0.0–1.1%) for wet and dry climates (IPCC, 2019b), respectively. However, under controlled environmental conditions of the present experiment, the amount of N supplied to the crop residue-amended soil could only partly explain the observed N_2O emissions (Table 1). In the present study, the average EF_{N2O} was 1.79% (−0.17 to 4.5%; Fig. 4C), which is beyond the uncertainty range of the disaggregated IPCC value (0.1–1.1%).

Furthermore, our MRA and PCA demonstrated that the maturity stage and the SWC and SWN fractions of the applied residue, rather than its total N content, are the major factors driving of the potential of the residue to promote soil N_2O emissions following incorporation (Table 2). Therefore, our findings suggest that the disaggregated EF_{N2O} for green vs. senescent crop residues depends on their biochemical characteristics. However, due to the limited number of residues investigated in the present study, providing such disaggregated factors may be inappropriate.

4.4. Effects of crop residue incorporation on soil NO emissions

NO released from aerobic soils is mainly produced through microbial nitrification (Russow et al., 2008), although it may also be produced through nitrifier denitrification (Medinets et al., 2015). A meta-analysis based on a limited number of studies, including some on crop

residue incorporation, reported that soil NO emissions mainly occurred following fertilizer application (Liu et al., 2017). In the present study, NO emissions did not occur in the first few days following residue incorporation, as in the case of N_2O, but they peaked approximately 2–3 weeks later, indicating that the observed stimulation of soil NO emissions was closely linked to residue decomposition, as no such peak was observed in the control treatment. Our stepwise MRA showed that the cumulative NO emissions were negatively correlated with the SWC and NH_4^+ content and positively correlated with the SOL-VS fraction of the residue (Table 1). Given this correlation and the delayed occurrence of the NO emission peak, we assume that either nitrification or nitrifier denitrification is the source of the observed NO emission. According to Wrage et al. (2001) nitrifier denitrification can serve as the key source of soil NO and N_2O emissions at high soil N availability but low soil organic C availability and O_2 pressure. However, as the NH_4^+ content of the residue was a negative predictor of cumulative NO emission, the importance of nitrifier denitrification as the driving process for NO peak emissions remains speculative. Given that the soil NO_3^- concentration continued to increase in our experiment following a first drop after the incorporation of residues, the most likely origin of the observed increase in NO emissions was nitrification. This assumption was further supported when the residue maturity stage was included in MRA and NH_4^+ became a significant positive predictor of NO emission (Table 2).

In the present study, the incorporation of crop residues stimulated soil NO emissions compared with the control treatment. Across six studies in a meta-analysis by Liu et al. (2017), residue incorporation reduced NO emissions by 9% on average. In contrast, Akiyama et al. (2020) reported that in a field study, the effects of residues on soil NO fluxes strongly differed among the residue types. For potato residues, Akiyama et al. (2020) calculated the annual EF_{NO} of 1.35%–2.44%, while cabbage residue produced no significant effect ($EF_{NO} \cong 0\%$). In the present study, the EF_{NO} over a 60-day period ranged from 0% for Po to 0.8% for Ry (Fig. 6B), and there was negative correlation between applied residue NH_4^+ and cumulative NO emissions (Table 1). Therefore, other residue characteristics, such as labile C fractions, should be considered in the estimations of regional or national NO emissions.

Overall, our results indicate that the incorporation of residue stimulates soil NO emissions over extended periods. This finding should be further investigated in field studies, specifically since the effects of residues on soil NO emissions remain relatively understudied and since the contribution of biogenic NO to the regional tropospheric NOx concentrations and, thus, to tropospheric O_3 formation, may be significant.

4.5. Crop residue incorporation increased NH_3 volatilization

NH_3 volatilization from crop residues is closely linked to residue decomposition, during which ammoniacal N is released, which is both a source of NH_3 and the starting point for a range of microbial processes, such as nitrification and denitrification, which can produce both NO and N_2O (Butterbach-Bahl et al., 2013). In a recent meta-analysis, Xia et al. (2018) pointed out that the application of residues to soils may be a major global source of atmospheric NH_3, although the magnitude of NH_3 volatilization due to residue management largely depends on soil texture and residue placement (e.g., mulch vs. plowing) rather than the residue type (Nett et al., 2016). In the present study, the incorporation of residue increased NH_3 volatilization by 25% on average, ranging between 2 and 6 kg N ha^{-1}, over 60 days (Appendix B, Fig. 1). Irrespective of the insignificant differences among crop residues in the present study, our MRA selected NH_4^+ as a significant predictor of NH_3 volatilization following the incorporation of crop residues (Tables 1, 2).

4.6. Cumulative gaseous N losses stimulated by incorporation of crop residue

Among the N gases studied (NO, N_2O, and NH_3), N_2O was on average (60%) the dominant N trace gas stimulated by residue incorporation

(Fig. 8). NH$_3$ emissions accounted for 31% of the mean value; however, depending on the residue type, NH$_3$ volatilization was reduced (Ry, WW, or RC).

The contribution of NO as an N loss pathway was relatively low and did not exceed 9% in any of the treatments. Presumably, the stimulation of denitrification after crop residue input (Li et al., 2016; Yamamoto et al., 2017) is the reason for the high N$_2$O emissions and the low NO emissions, as NO is mainly formed during nitrification (Medinets et al., 2015). The fractionation between NO and N$_2$O was not significantly modulated by the biochemical composition (soluble, cellulose, and lignin-like fractions) of the residues. Following the stepwise selection in MRA, the NO$_3^-$ content of the residue was the most important predictor of the ratio of N$_2$O:NO emissions.

According to a recent field study, WFPS is an important controlling factor for NO emissions after residue input (Akiyama et al., 2020). In general, nitrification is the predominant process when the WFPS is below 60%, whereas denitrification becomes predominant when the WFPS exceeds 60% (Pilegaard, 2013). In the present study, soil was maintained at 60% WFPS; thus, the ratio of N$_2$O:NO emission was expected to be close to 1. However, NO made the smallest contribution to the reactive gaseous N loss in our experiment. Cumulative gaseous reactive N loss (N$_2$O + NO+NH$_3$) was strongly promoted by SOL-VS, CEL, HEM, and NH$_4^+$ of the residues (Table 1). Furthermore, the importance of the maturity stage of the residues for gaseous N loss was proven again when it was included as a variable in the multiple regression model (Table 2). Despite the lower explanatory power of the resulting model, the crop maturity stage as a single variable could be used as a simple classification scheme. Likewise, the predicted combined cumulative emission (N$_2$O + NO) from residue recycling was very well (R^2 = 0.838, Table 2) according to the following multiple linear regression model:

$$N2O + NO = 9.04 + 3.98 \times \mathbf{maturity[green]} + 8.36 \times \mathbf{SWN} - 1.18 \\ \times \mathbf{SWC} - 0.09 \times \mathbf{HEM} - 0.33 \times \mathbf{LIG}$$

Overall, our results indicate that maturity can be used as a key predictor of the potential of a residue to stimulate soil gaseous reactive N loss, although additional experiments with other soil types are warranted for validation. Rather than the N content or C/N ratio of the applied residue, the readily available SWC and SWN fractions positively or negatively control the combined emission of N$_2$O and NO. Further, the HEM and LIG fractions in the residue material play additional roles in controlling these emissions.

4.7. Limitations of the incubation approach

Although the present study furthered our understanding of the effects of the maturity stage and biochemical composition of residues on soil N trace gas emissions, the incubation approach has a few limitations. Briefly, the experiments were conducted with re-packed soil columns, which reduces the variability of soil physicochemical characteristics usually observed in situ. While working with sieved and re-packed soils usually ensures an initial even distribution of microbes and a high probability that they can access their substrates (Schnecker et al., 2019), it also results in artifacts, such as increased microbial activity. Moreover, re-wetting of dried soils further stimulates microbial activity, resulting in a pulse of C and N mineralization (Borken and Matzner, 2009). Furthermore, our experiment only included a single soil type, even though the effect of residue incorporation on soil N$_2$O emissions may vary depending on soil properties, such as texture (Charles et al., 2017). Finally, soil mesocosms were incubated under standardized moisture and temperature, although these conditions greatly vary in the field. Adjusting temperature and soil moisture to the target values is usually followed by a period of marked changes in soil microbial activity and soil C and N trace gas fluxes. Therefore, we set a pre-incubation period of a week, such that the effects of re-wetting on soil microbial activity were mostly diminished, as evidenced by the decline in soil respiration (Appendix B, Fig. 2). Therefore, our results regarding the magnitude of the effects of residues on soil C and N trace gas emissions are not directly transferable to the field situation. Nonetheless, the incubation approach allowed us to closely monitor and quantify the effects and mechanisms of residue incorporation on soil N trace gas losses as well as soil microbial C and N turnover processes, although the latter remain to be explored. Working with intact soil cores may further improve the transferability of results to field situations. However, this would introduce an additional
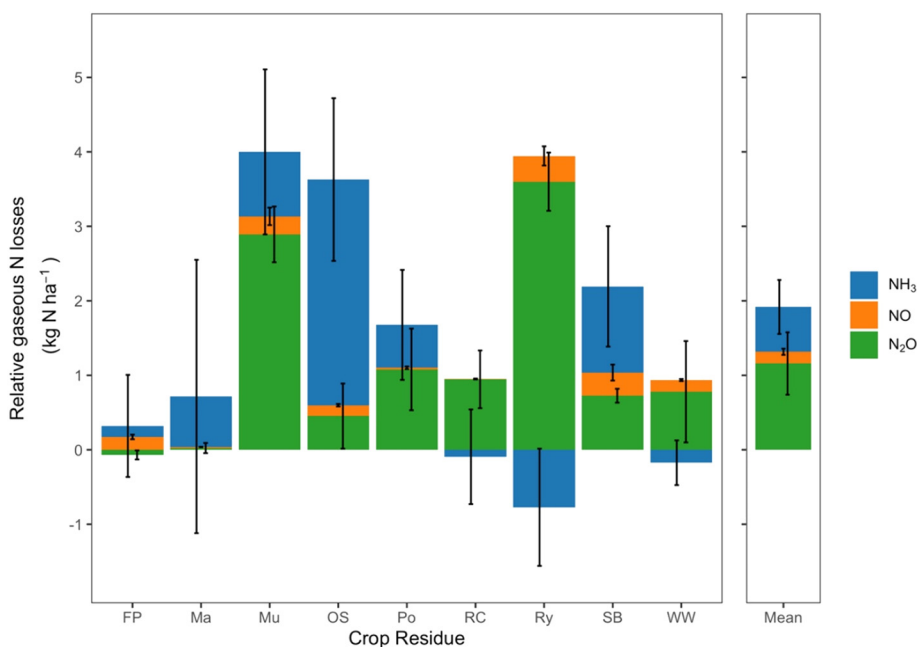
Fig. 8. Gaseous N (N$_2$O, NO, and NH$_3$) losses (mean ± SE; n = 3) from soil cores with residue incorporation (4 t DW ha^{-1}) relative to the control without residue incorporation over a 60-day incubation period. FP: field pea; Ma: maize; Mu: mustard; OS: oilseed rape; Po: potato; RC: red clover; Ry: ryegrass; SB: sugar beet; WW: winter wheat. Overall mean ± SE (n = 9), excluding Co, is shown.

level of complexity due to small scale soil inhomogeneities, which obviously already hamper the identification of the effects of residue incorporation on soil N emissions in the field (Arias-Navarro et al., 2017; Clemens et al., 1999; Kravchenko et al., 2017). Furthermore, future studies should explore additional N loss pathways through similar mesocosm experiments. Specifically, the effects of residue incorporation on NO_3^- leaching and dinitrogen (N_2) emissions via denitrification should be investigated. While hydrological N losses can be quantified easily in mesocosm experiments, reliable quantification of soil N_2 emissions remains a challenge both under field and laboratory conditions (Wang et al., 2020). However, quantifying N_2 emissions is a prerequisite to close the N-balance; thus, to better understand the effects of residues on soil N cycling and environmental N losses, this loss pathway should be quantified (Zistl-Schlingmann et al., 2019).

5. Conclusion

The current national emission inventory methods use a direct EF_{N2O}, with a single default value of 1%, for N input from organic amendments. The 2019 amendment of the IPCC guidelines specified the EF_{N2O} value for crop residues is 0.5–0.6% (IPCC, 2019b). However, in the present incubation experiment, the average EF_{N2O} values for nine different crop residues were beyond the given uncertainty rage of 1.79 ± 0.3%. Therefore, the N content or C/N ratio of the applied residue alone is not sufficient to explain the variations in N_2O emissions. Additional biochemical components, including the soluble, cellulose, and lignin fractions, as well as the maturity stage of the incorporated residue were analyzed to explore their relationships with the soil N_2O, NO, and NH_3 emissions. The residue maturity stage may be used as a simple proxy for gaseous N losses in clayey loamy soils. Our findings suggest a further disaggregation of the EF_{N2O} approach, that is, differentiation between the green (i.e., photosynthetic active) and senescent (e.g., straw) stages and consideration of the biochemical properties of the residues. The proposed EF_{N2O} approach can contribute to the improved reporting of GHG emissions from crop residues in national inventories in the coming years. Nevertheless, further investigations on the comparability of the results obtained with re-packed soil columns and those obtained from in situ studies are recommended. While the incorporation of crop residues arguably stimulates the emission of N trace gases from agricultural soils, this amendment is essential to maintain or further improve soil C stocks and soil fertility as well as crop yield. Careful residue management can help avoid potentially high N losses from their input, such as through delayed incorporation or drying.

Funding

CRediT authorship contribution statement

Baldur Janz: Writing – original draft, Investigation, Formal analysis, Visualization. **Felix Havermann:** Software, Methodology, Investigation, Formal analysis. **Gwenaëlle Lashermes:** Writing – review & editing, Investigation. **Pablo Zuazo:** Methodology. **Florian Engelsberger:** Methodology. **Seyedeh Mahsa Torabi:** Investigation. **Klaus Butterbach-Bahl:** Conceptualization, Writing – review & editing, Funding acquisition.

Declaration of competing interest

The authors declare that they have no known competing financial interests or personal relationships that could have appeared to influence the work reported in this paper.

Acknowledgements

Supplementary data

References

AFNOR, 2004. French Standard NF EN 12260, Water Quality - Determination of Nitrogen - Determination of Bound Nitrogen (TN sub b), Following Oxidation to Nitrogen Oxides. AFNOR, Paris.

Akiyama, H., Yamamoto, A., Uchida, Y., Hoshino, Y.T., Tago, K., Wang, Y., Hayatsu, M., 2020. Effect of low C/N crop residue input on N2O, NO, and CH4 fluxes from andosol and fluvisol fields. Sci. Total Environ. 713, 1–10. https://doi.org/10.1016/j.scitotenv.2020.136677.

Arias-Navarro, C., Díaz-Pinés, E., Klatt, S., Brandt, P., Rufino, M.C., Butterbach-Bahl, K., Verchot, L.V., 2017. Spatial variability of soil N2O and CO2 fluxes in different topographic positions in a tropical montane forest in Kenya. J. Geophys. Res. Biogeosci. 122, 514–527. https://doi.org/10.1002/2016JG003667.

Baggs, E.M., Watson, C.A., Rees, R.M., 2000. The fate of nitrogen from incorporated cover crop and green manure residues. Nutr. Cycl. Agroecosyst. 56, 153–163. https://doi.org/10.1023/A:1009825606341.

Bobbink, R., Heil, G.W., Raessen, M.B.A.G., 1992. Atmospheric deposition and canopy exchange processes in heathland ecosystems. Environ. Pollut. 75, 29–37. https://doi.org/10.1016/0269-7491(92)90053-D.

Bolleter, W.T., Bushman, C.J., Tidwell, P.W., 1961. Spectrophotometric determination of ammonia as indophenol. Anal. Chem. 33, 592–594. https://doi.org/10.1021/ac60172a034.

Borken, W., Matzner, E., 2009. Reappraisal of drying and wetting effects on C and N mineralization and fluxes in soils. Glob. Chang. Biol. 15, 808–824. https://doi.org/10.1111/j.1365-2486.2008.01681.x.

Butterbach-Bahl, K., Gasche, R., Breuer, L., Papen, H., 1997. Fluxes of NO and N2O from temperate forest soils: impact of forest type, N deposition and of liming on the NO and N2O emissions. Nutr. Cycl. Agroecosyst. 48, 79–90. https://doi.org/10.1023/A:1009785521107.

Butterbach-Bahl, K., Kahl, M., Mykhayliv, L., Werner, C., Kiese, R., Li, C, 2009. A european-wide inventory of soil NO emissions using the biogeochemical models DNDC/Forest-DNDC. Atmos. Environ. 43, 1392–1402. https://doi.org/10.1016/j.atmosenv.2008.02.008.

Butterbach-Bahl, K., Baggs, E.M., Dannenmann, M., Kiese, R., Zechmeister-Boltenstern, S., 2013. Nitrous oxide emissions from soils: how well do we understand the processes and their controls? Philos. Trans. R. Soc. Lond. Ser. B Biol. Sci. 368, 20130122. https://doi.org/10.1098/rstb.2013.0122.

Charles, A., Rochette, P., Whalen, J.K., Angers, D.A., Chantigny, M.H., Bertrand, N., 2017. Global nitrous oxide emission factors from agricultural soils after addition of organic amendments: a meta-analysis. Agric. Ecosyst. Environ. 236, 88–98. https://doi.org/10.1016/j.agee.2016.11.021.

Chen, H., Li, X., Hu, F., Shi, W., 2013. Soil nitrous oxide emissions following crop residue addition: a meta-analysis. Glob. Chang. Biol. 19, 2956–2964. https://doi.org/10.1111/gcb.12274.

Ciais, P., Sabine, C., Bala, G., Bopp, L., Brovkin, V., Canadell, J., Chhabra, A., DeFries, R., Galloway, J., Heimann, M., Jones, C., Quéré, C.Le, Myneni, R.B., Piao, S., Thornton, P., 2013. The physical science basis. Contribution of working group I to the fifth assessment report of the intergovernmental panel on climate change. Chang. IPCC Clim. 465–570. https://doi.org/10.1017/CBO9781107415324.015.

Clemens, J., Schillinger, M.P., Goldbach, H., Huwe, B., 1999. Spatial variability of N2O emissions and soil parameters of an arable silt loam – a field study. Biol. Fertil. Soils 28, 403–406. https://doi.org/10.1007/s003740050512.

Devêvre, O.C., Horwáth, W.R., 2000. Decomposition of rice straw and microbial carbon use efficiency under different soil temperatures and moistures. Soil Biol. Biochem. 32, 1773–1785. https://doi.org/10.1016/S0038-0717(00)00096-1.

Francis, D.D., Vigil, M.F., Mosier, A.R., 2008. Gaseous losses of nitrogen other than through denitrification. Nitrogen in Agricultural Systems, Agronomy Monograph. 49, pp. 255–279. https://doi.org/10.2134/agronmonogr49.c8.

Goering, H.K., Van Soest, P.J., 1970. Forage Fiber Analyses: (Apparatus, Reagents, Procedures, and Some Applications), Agricultural Research Service. U.S. Dept. of Agriculture, Washington, D.C.

Huang, Y., Zou, J., Zheng, X., Wang, Y., Xu, X., 2004. Nitrous oxide emissions as influenced by amendment of plant residues with different C: N ratios. Soil Biol. Biochem. 36, 973–981. https://doi.org/10.1016/j.soilbio.2004.02.009.

Ingwersen, J., Butterbach-Bahl, K., Gasche, R., Richter, O., Papen, H., 1999. Barometric process separation: new method for quantifying nitrification, denitrification, and nitrous oxide sources in soils. Soil Sci. Soc. Am. J. 63, 117–128. https://doi.org/10.2136/sssaj1999.03615995006300010018x.

IPCC, 2006. 2006 IPCC Guidelines for National Greenhouse Gas Inventories, Chapter 5 Cropland.

IPCC, 2019a. In: Shukla, R. Skea, Buendia, J., Masson-Delmotte, E. Calvo, IPCC, V. (Eds.), Special Report on Climate Change and Land: Summary for Policyakers, Climate Change and Land: An IPCC Special Report on Climate Change, Desertification, Land

ARTICLE IN PRESS

B. Janz, F. Havermann, G. Lashermes et al.   Science of the Total Environment xxx (xxxx) xxx

Degradation, Sustainable Land Management, Food Security, and Greenhouse Gas Fluxes in Terrestrial Ecosystems https://doi.org/10.1002/9781118786352.wbieg0538.

IPCC, 2019b. 2019 Refinement to the 2006 IPCC Guidelines for National Greenhouse Gas Inventories. Chapter 11. N2O Emissions from Managed Soils, and CO2 Emissions from Lime and Urea Application.

Kravchenko, A.N., Toosi, E.R., Guber, A.K., Ostrom, N.E., Yu, J., Azeem, K., Rivers, M.L., Robertson, G.P., 2017. Hotspots of soil N2O emission enhanced through water absorption by plant residue. Nat. Geosci. 10, 496–500. https://doi.org/10.1038/ngeo2963.

Kriaučiuniene, Z., Velička, R., Raudonius, S., 2012. The influence of crop residues type on their decomposition rate in the soil: a litterbag study. Zemdirbyste 99, 227–236.

Kuzyakov, Y., Blagodatskaya, E., 2015. Microbial hotspots and hot moments in soil: Concept & review. Soil Biol. Biochem. 83, 184–199. https://doi.org/10.1016/j.soilbio.2015.01.025.

Lashermes, G., Nicolardot, B., Parnaudeau, V., Thuriès, L., Chaussod, R., Guillotin, M.L., Linères, M., Mary, B., Metzger, L., Morvan, T., Tricaud, A., Villette, C., Houot, S., 2010. Typology of exogenous organic matters based on chemical and biochemical composition to predict potential nitrogen mineralization. Bioresour. Technol. 101, 157–164. https://doi.org/10.1016/j.biortech.2009.08.025.

Lehtinen, T., Schlatter, N., Baumgarten, A., Bechini, L., Krüger, J., Grignani, C., Zavattaro, L., Costamagna, C., Spiegel, H., 2014. Effect of crop residue incorporation on soil organic carbon and greenhouse gas emissions in European agricultural soils. Soil Use Manag. 30, 524–538. https://doi.org/10.1111/sum.12151.

Li, X., Hu, F., Shi, W., 2013. Plant material addition affects soil nitrous oxide production differently between aerobic and oxygen-limited conditions. Appl. Soil Ecol. 64, 91–98. https://doi.org/10.1016/j.apsoil.2012.10.003.

Li, X., Sørensen, P., Olesen, J.E., Petersen, S.O., 2016. Evidence for denitrification as main source of N2O emission from residue-amended soil. Soil Biol. Biochem. 92, 153–160. https://doi.org/10.1016/j.soilbio.2015.10.008.

Li, F., Sørensen, P., Li, X., Olesen, J.E., 2020. Carbon and nitrogen mineralization differ between incorporated shoots and roots of legume versus non-legume based cover crops. Plant Soil 446, 243–257. https://doi.org/10.1007/s11104-019-04358-6.

Liu, C., Lu, M., Cui, J., Li, B., Fang, C., 2014. Effects of straw carbon input on carbon dynamics in agricultural soils: a meta-analysis. Glob. Chang. Biol. 20, 1366–1381. https://doi.org/10.1111/gcb.12517.

Liu, S., Lin, F., Wu, S., Ji, C., Sun, Y., Jin, Y., Li, S., Li, Z., Zou, J., 2017. A meta-analysis of fertilizer-induced soil NO and combined NO+N2O emissions. Glob. Chang. Biol. 23, 2520–2532. https://doi.org/10.1111/gcb.13485.

Liu, M., Huang, Xin, Song, Y., Tang, J., Cao, J., Zhang, X., Zhang, Q., Wang, S., Xu, T., Kang, L., Cai, X., Zhang, H., Yang, F., Wang, H., Yu, J.Z., Lau, A.K.H., He, L., Huang, Xiaofeng, Duan, L., Ding, A., Xue, L., Gao, J., Liu, B., Zhu, T., 2019. Ammonia emission control in China would mitigate haze pollution and nitrogen deposition, but worsen acid rain. Proc. Natl. Acad. Sci. U. S. A. 116, 7760–7765. https://doi.org/10.1073/pnas.1814880116.

Lugato, E., Bampa, F., Panagos, P., Montanarella, L., Jones, A., 2014. Potential carbon sequestration of European arable soils estimated by modelling a comprehensive set of management practices. Glob. Chang. Biol. 20, 3557–3567. https://doi.org/10.1111/gcb.12551.

Malique, F., Ke, P., Boettcher, J., Dannenmann, M., Butterbach-Bahl, K., 2019. Plant and soil effects on denitrification potential in agricultural soils. Plant Soil 439, 459–474. https://doi.org/10.1007/s11104-019-04038-5.

Medinets, S., Skiba, U., Rennenberg, H., Butterbach-Bahl, K., 2015. A review of soil NO transformation: Associated processes and possible physiological significance on organisms. Soil Biol. Biochem. 80, 92–117. https://doi.org/10.1016/j.soilbio.2014.09.025.

Nemitz, E., Dorsey, J.R., Flynn, M.J., Gallagher, M.W., Hensen, A., Erisman, J.W., Owen, S.M., Dämmgen, U., Sutton, M.A., 2009. Aerosol fluxes and particle growth above managed grassland. Biogeosciences 6, 1627–1645. https://doi.org/10.5194/bg-6-1627-2009.

Nett, L., Sradnick, A., Fuß, R., Flessa, H., Fink, M., 2016. Emissions of nitrous oxide and ammonia after cauliflower harvest are influenced by soil type and crop residue management. Nutr. Cycl. Agroecosyst. 106, 217–231. https://doi.org/10.1007/s10705-016-9801-2.

Pilegaard, K., 2013. Processes regulating nitric oxide emissions from soils. Philos. Trans. R. Soc. Lond. Ser. B Biol. Sci. 368. https://doi.org/10.1098/rstb.2013.0126.

Pugesgaard, S., Petersen, S.O., Chirinda, N., Olesen, J.E., 2017. Crop residues as driver for N2O emissions from a sandy loam soil. Agric. For. Meteorol. 233, 45–54. https://doi.org/10.1016/j.agrformet.2016.11.007.

Rennenberg, H., Gessler, A., 1999. Consequences of N deposition to forest ecosystems - recent results and future research needs. Water Air Soil Pollut. 116, 47–64.

Robertson, G.P., Groffman, P.M., 2015. Nitrogen transformations. In: Paul, E.A. (Ed.), Soil Microbiology, Ecology and Biochemistry, Third edition Academic Press, Burlington, Massachusets, USA, pp. 421–446 https://doi.org/10.1016/b978-0-12-415955-6.00014-1.

Russow, R., Spott, O., Stange, C.F., 2008. Evaluation of nitrate and ammonium as sources of NO and N2O emissions from black earth soils (Haplic Chernozem) based on 15N field experiments. Soil Biol. Biochem. 40, 380–391. https://doi.org/10.1016/j.soilbio.2007.08.020.

Schmatz, R., Recous, S., Aita, C., Tahir, M.M., Schu, A.L., Chaves, B., Giacomini, S.J., 2017. Crop residue quality and soil type influence the priming effect but not the fate of crop residue C. Plant Soil 414, 229–245. https://doi.org/10.1007/s11104-016-3120-x.

Schnecker, J., Bowles, T., Hobbie, E.A., Smith, R.G., Grandy, A.S., 2019. Substrate quality and concentration control decomposition and microbial strategies in a model soil system. Biogeochemistry 8, 47–59. https://doi.org/10.1007/s10533-019-00571-8.

Surey, R., Schimpf, C.M., Sauheitl, L., Mueller, C.W., Rummel, P.S., Dittert, K., Kaiser, K., Böttcher, J., Mikutta, R., 2020. Potential denitrification stimulated by water-soluble organic carbon from plant residues during initial decomposition. Soil Biol. Biochem. 147. https://doi.org/10.1016/j.soilbio.2020.107841.

Van Der Eerden, L., De Vries, W., Van Dobben, H., 1998. Effects of ammonia deposition on forests in the Netherlands. Atmos. Environ. 32, 525–532. https://doi.org/10.1016/S1352-2310(97)00009-5.

Van Soest, P.J., McQueen, R.W., 1973. The chemistry and estimation of fibre. Proc. Nutr. Soc. 32, 123–130. https://doi.org/10.1079/pns19730029.

Vanlauwe, B., Nwoke, O.C., Sanginga, N., Merckx, R., 1996. Impact of residue quality on the C and N mineralization of leaf and root residues of three agroforestry species. Plant Soil 183, 221–231. https://doi.org/10.1007/BF00011437.

Wang, R., Pan, Z., Zheng, X., Ju, X., Yao, Z., Butterbach-Bahl, K., Zhang, C., Wei, H., Huang, B., 2020. Using field-measured soil N2O fluxes and laboratory scale parameterization of N2O/(N2O+N2) ratios to quantify field-scale soil N2 emissions. Soil Biol. Biochem. 148, 107904. https://doi.org/10.1016/j.soilbio.2020.107904.

Wrage, N., Velthof, G.L., Van Beusichem, M.L., Oenema, O., 2001. Role of nitrifier denitrification in the production of nitrous oxide. Soil Biol. Biochem. 33, 1723–1732. https://doi.org/10.1016/S0038-0717(01)00096-7.

Xia, L., Lam, S.K., Wolf, B., Kiese, R., 2018. Trade-offs between soil carbon sequestration and reactive nitrogen losses under straw return in global agroecosystems. Glob. Chang. Biol. https://doi.org/10.1111/gcb.14466.

Yamamoto, A., Akiyama, H., Nakajima, Y., Hoshino, Y.T., 2017. Estimate of bacterial and fungal N2O production processes after crop residue input and fertilizer application to an agricultural field by 15N isotopomer analysis. Soil Biol. Biochem. 108, 9–16. https://doi.org/10.1016/j.soilbio.2017.01.015.

Yansheng, C., Fengliang, Z., Zhongyi, Z., Tongbin, Z., Huayun, X., 2020. Biotic and abiotic nitrogen immobilization in soil incorporated with crop residue. Soil Tillage Res. 202. https://doi.org/10.1016/j.still.2020.104664.

Zistl-Schlingmann, M., Feng, J., Kiese, R., Stephan, R., Zuazo, P., Willibald, G., Wang, C., Butterbach-Bahl, K., Dannenmann, M., 2019. Dinitrogen emissions: an overlooked key component of the N balance of montane grasslands. Biogeochemistry https://doi.org/10.1007/s10533-019-00547-8.